A MEASUREMENT OF THE RATIO OF CHARGE TO MASS OF FREE ELECTRONS USING A RESONANT CAVITY

Thesis by

Charles Harold Wilts

In Partial Fulfillment of the Requirements

For the Degree of

Doctor of Philosophy

California Institute of Technology

Pasadena, California

1948

ACKNOWLEDGEMENT

This work was carried out under
the helpful supervision of Professor
W. R. Smythe

ABSTRACT

A deflection method for measuring (e/m_0) for free electrons is described. A beam of electrons is directed along the axis of a cylindrical cavity excited in the TM_{110} mode. A null in the subsequent deflection of the beam occurs when the transit time is nearly equal to an integral number of cycles of the cavity oscillation. The average velocity of the electron beam is calculated from knowledge of the cavity dimensions and the resonant frequency of the cavity. The value of (e/m_0) is obtained by equating the energy required to accelerate the electrons and their kinetic energy. Three quantities must be measured, a distance, a frequency and a difference of potential, and two very small corrections must be made. Errors due to unmeasurable work function potentials, etc., are eliminated by taking two sets of data with different transit times and subtracting the two energy equations. A probable error of less than 1 part in 10,000 seems to be achievable. Preliminary apparatus gave a value

$$e/m_0 = 1.759 \pm .007 \quad (10)^7 \quad \text{emu per gram.}$$

TABLE OF CONTENTS

LIST OF ILLUSTRATIONS

I. INTRODUCTION

The ratio of charge to mass for the electron has long been recognized as an important physical constant. Two general methods have been developed for the measurement of this quantity. One perhaps the more fundamental, utilizes free electrons which are deflected in a calculable manner by electromagnetic fields. The other utilizes spectroscopic phenomena of bound electrons such as the fine structure and Zeeman effect which can be calculated quantitatively in terms of the value of e/m.

Determinations of increasing precision have been made during the past 50 years. Probable errors for deflection methods have been stated to be of the order of 1 part in 1000, although it is now believed that no determinations except those of Kirchner(1) and Dunnington(2) achieved such accuracy. Indeed Dunnington is the only one to claim a probable error appreciably better than 1 part in 1000, his value being given at 2 parts in 10,000. Because his determination required the use of relatively large estimated corrections, another method capable of equal apparent precision or of course of even greater precision is of importance. It is the purpose of this thesis to describe a new method which seems to offer promise of achieving this.

Earlier methods have had various limitations and difficulties. Among these are the following:

1. Measurements of electron potential have involved corrections for work function, contact potential, and initial electron velocities which were only approximately known.
2. Some methods have involved production of a uniform and known magnetic field over a large region which is quite difficult to achieve with great accuracy.
3. Electron bombardment of metal surfaces gives rise to peculiar

insulating layers which when charged influence the motion of electron beams nearby. This seems to have been a common source of error.

The present method has eliminated all such difficulties and indeed it appears that there are only three very small corrections requiring consideration. All of these are either negligible or can be calculated with sufficient precision to permit high accuracy.

II THEORY

Basically, this method is similar to that of Kirchner(3) or Perry and Chaffee(4). The electron velocity and potential are measured and then related by the expression

$$(2.1) \qquad eV = m_0c^2\left\{\frac{1}{(1 - v^2/c^2)^{1/2}} - 1\right\}.$$

This method is a true deflection method, however, since the velocity is measured by observing a deflection effect of an electromagnetic field.

One of the most sharply bounded electromagnetic fields is that within a resonant cavity. Not only is the boundary region very narrow, but the field configuration within the cavity is accurately known. Consider a cylindrical cavity of radius (a) and length (d) excited in the TM_{110} mode. In cylindrical coordinates, the electric field is given by the expression:

$$(2.2) \qquad \bar{E} = -\frac{2\omega B_0}{kc}\left[\, J_1(k\rho)\cos\phi \,\right]\sin\omega t\ \bar{k}_1$$

and the magnetic induction by:

$$(2.3) \qquad \bar{B} = 2B_0\left[\bar{\rho}_1\frac{J_1(k\rho)}{k\rho}\sin\phi + \bar{\phi}_1\, J_1'(k\rho)\cos\phi\right]\cos\omega t$$

where

$$J_1(ka) = 0 \qquad \text{and} \qquad 0 < z < d\ .$$

See Figure 1. These values are independent of z. In the neighborhood of $\bar{\rho} = 0$, the fields are $\bar{E} = 0$ and $\bar{B} = B_0\cos\omega t\ \bar{j}_1$, the latter being a uniform magnetic field directed along the y axis.

An electron with initial velocity $\bar{v}_0$ directed along the z axis will be acted upon by a force given in general by

$$(2.4) \qquad \bar{F} = m\bar{a} = -\frac{e}{c}\ \bar{v} \times \bar{B}\ .$$

In rectangular coordinates, the differential equations of motion are

$$(2.5) \qquad \ddot{y} = 0 \qquad \ddot{z} = -\frac{e}{mc}\,\dot{x}\,B_0\cos\omega t \qquad \ddot{x} = \frac{e}{mc}\,\dot{z}\,B_0\cos\omega t$$

FIGURE 1

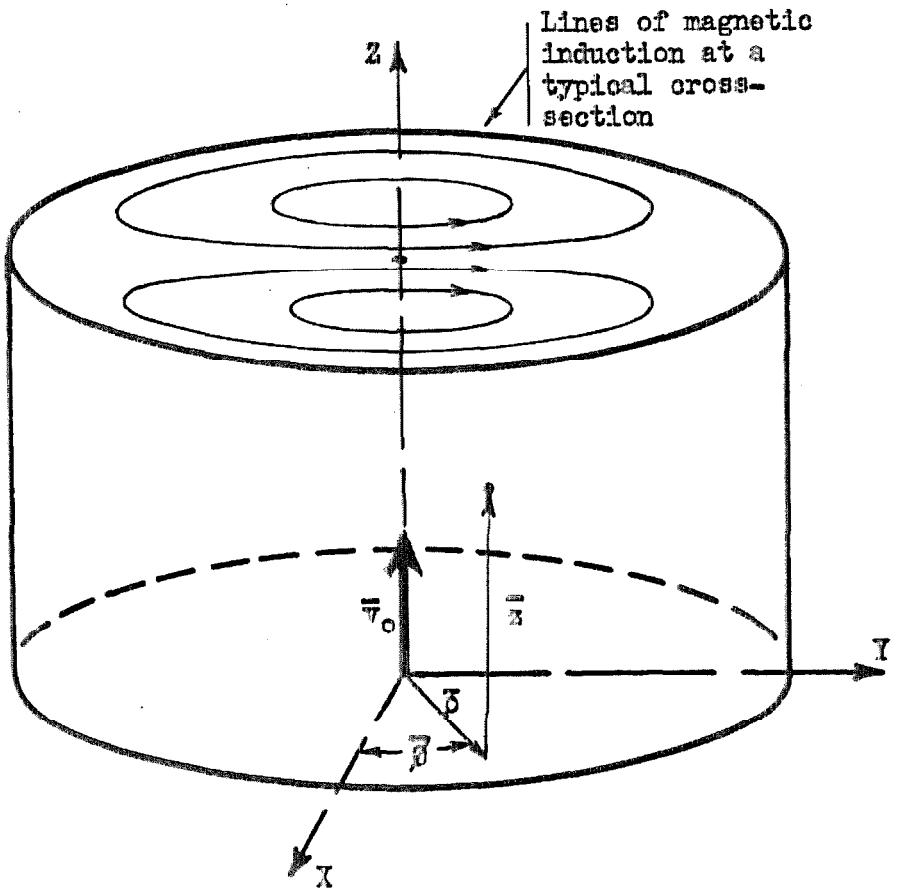

1. Coordinate System for Analysis of Electron Trajectories in Cylindrical Cavity Excited in TM_{110} Mode

with initial conditions at time t_1 when the electron enters the field

$$\dot{x}_1 = x_1 = \dot{y}_1 = y_1 = z_1 = 0 \quad ; \quad \dot{z}_1 = v_0 .$$

Separation of dependent variables and setting $\frac{e}{mc}\frac{B_0}{\omega} = \beta$ give identical equations for x and z :

$$(2.6) \qquad \dddot{x} + \ddot{x}\,\omega \tan \omega t + \frac{\beta^2}{\omega^2}\,\dot{x}\,\cos^2\omega t = 0 .$$

This equation is most readily solved by making the substitution $v = \sin \omega t$. Integration of the resulting equation and substitution of the given initial conditions give

$$(2.7) \qquad \dot{x} = v_0 \sin\left[\beta(\sin \omega t - \sin \omega t_1)\right]$$

$$(2.8) \qquad \dot{z} = v_0 \cos\left[\beta(\sin \omega t - \sin \omega t_1)\right] .$$

Further integration of these equations in terms of elementary functions is impossible. However, since β is a very small number for practicable values of the magnetic induction, x and z can be obtained with good precision by expansion of the trigonometric terms in power series, and integration of the first few terms. This gives

$$(2.9) \qquad x = -\frac{\beta v_0}{\omega}\left[(\cos \omega t - \cos \omega t_1) + \omega(t-t_1)\sin \omega t_1\right]$$

$$(2.10) \qquad z = v_0(t-t_1)\left[1 - \beta^2(1 - \tfrac{1}{2}\cos 2\omega t_1)\right]$$
$$- \beta^2 v_0/2\omega\left[\sin \omega t \cos \omega t - 4 \cos \omega t \sin \omega t_1 + 3 \sin \omega t_1 \cos \omega t_1\right].$$

In a later discussion it will be necessary to consider all terms in these equations, but for a preliminary discussion of the theory it is sufficient to consider (2.7) , (2.9) and the approximate equation:

$$(2.11) \qquad z = v_0(t-t_1)(1-\beta^2) .$$

When the electron leaves the cavity, $z_2 = d$ and $t_2 = t_1 + \nu$ where ν is the "transit time". Thus from (2.11) the transit time is given by

$$(2.12) \qquad \nu = \frac{d}{v_0(1-\beta^2)} .$$

and Equations (2.7) and (2.9) can be rewritten in the following form:

$$(2.13) \qquad \dot{x}_2 = v_0 \sin 2\beta \sin(\omega\nu/2) \cos \omega(t_1+\nu/2)$$

$$(2.14) \qquad x_2 = 2\beta v_0/\omega \left\{\sin(\omega\nu/2) \sin \omega(t_1+\nu/2) - \omega\nu/2 \sin \omega t_1\right\}.$$

It can be seen from equations (2.7) and (2.8) that the electron velocity remains constant, but the direction varies with time. However the angle between the velocity vector and the z axis is always very small. If the electron is permitted to travel through field free space for a distance (L) , the total deflection at right angles to the direction of motion is

$$(2.15) \qquad x' = \dot{x}_2 L/v_0 + x_2$$
$$= 2\beta L\left\{\sin \omega\nu/2 \left[\cos \omega(t_1+\nu/2) + v_0/\omega L \sin \omega(t_1+\nu/2)\right] - d/2L \sin \omega t_1\right\}.$$

Neglecting for simplicity the last two terms we have the approximate equation

$$(2.16) \qquad x' = 2\beta L \sin \omega\nu/2 \cos \omega(t_1+\nu/2) .$$

The deflection x' depends on the quantity (β) which is a measure of the field strength, and in addition on the time of entry t_1 and the transit time ν. The important fact is that x' is zero for all values of t_1 and (βL) if and only if the transit time is an integral number of periods of the cavity oscillation, that is $\omega\nu = 2\pi n$. For other values of the transit time the electron is deflected by an amount depending on the entry time, but lying within the limits $\pm 2\beta L \sin \omega\nu/2$. Considering now an electron beam instead of a single electron, it is apparent that the beam will be spread out into a "fan", the angular spread of which will be $2\beta \sin \omega\nu/2$ radians, and only when $\omega\nu = 2\pi n$ will the spread be zero.

This provides a method for measuring the electron velocity, for if the electron velocity can be adjusted so that the angular spread is zero, then the initial velocity according to equation (2.12) is

(2.15) $v_1 = d/\nu(1-\beta^2) = d\omega/2n_1\pi(1-\beta^2)$

where only the integer n_1 is unknown. If now the electron velocity is varied until the angular spread again becomes zero, a similar equation holds

(2.16) $v_2 = d\omega/2n_2\pi(1-\beta^2)$.

If the potential through which the electron has fallen in the two cases is V_1 and V_2 respectively, then one obtains from equation (2.1) the following equation for e/m_0 :

$$(2.17) \qquad e/m_0 = c^2 \left\{ \frac{\frac{1}{(1 - v_2^2/c^2)^{1/2}} - \frac{1}{(1 - v_1^2/c^2)^{1/2}}}{V_2 - V_1} \right\}.$$

Where v_1 and v_2 are given above. If $v_2/c \ll 1$, so that the relativistic energy equation need not be used, the equation for e/m_0 becomes

$$(2.18) \qquad e/m_0 = \frac{\omega^2 d^2}{8\pi^2} \left(\frac{1/n_2^2 - 1/n_1^2}{V_2 - V_1} \right) \frac{1}{(1-\beta^2)^2} .$$

Equation (2.10) for velocity is not exact because the electric field is not zero the magnetic field not uniform if the electron is displaced from the z axis. Consequently both the lateral motion and motion along the z axis are modified slightly. These effects are very small and will be considered later.

III. DETECTION

In the previous section it was shown that the deflection of the electron beam produced at the end of the drift region by the cavity field is

$$x' = 2\beta L \sin(\omega\nu/2) \cos \omega(t_1+\nu/2) + \Delta \tag{3.1}$$

where Δ includes two small terms that will be considered later. The problem of detection is to determine in some manner an accelerating potential which gives rise to zero deflection of the electron beam, or more correctly on making allowance for the term Δ a minimum deflection.

Two methods of finding a minimum of this deflection have been used. If the beam is allowed to fall on a fluorescent screen, the "spread" can be readily observed and the voltage can be adjusted so that this spread is a minimum. Another method involves measurement of that part of the beam current which passes through another slit at the end of the drift region. Assume for simplicity that the electron beam is of uniform density and of width (h). Consider a slit also of width (h) placed at the end of the drift path so that the entire beam passes through the slit when it is undeflected. If the beam is deflected by an amount less than (h), only a part of the beam will pass through the slit, and if the deflection is more than (h), none of the beam will pass through. Since cavity excitation will produce a sinusoidal deflection of the beam, the average current passing through the slit will depend on the cavity excitation and the transit time. It is shown in Appendix II that if the total current of the beam is I_0, the current passing through the slit will be:

$$\begin{aligned} I &= I_0(1-(2/\pi)\gamma) && \text{for } \gamma \leqslant 1 \\ I &= I_0(2/\pi)\left[\sin^{-1}(1/\gamma) - \gamma + \sqrt{\gamma^2+1}\right] && \text{for } \gamma > 1 \end{aligned} \tag{3.2}$$

where $\gamma = x'_{max}/n = (2\beta L/h)\sin(\omega\nu/2)$.

It can be seen from equation (3.2) that if $\beta L/h \gg 1$ then the region where $\gamma \leq 1$ lies in a very small range of $\omega\nu$ so that $\sin(\omega\nu/2)$ varies nearly linearly with ν. Thus the current I also varies nearly linearly with ν near the transit time $\nu = 2n\pi/\omega$. This linearity extends to the points corresponding to $\left|\omega\nu/2 - 2n\pi\right| = \frac{1}{2\beta L/h}$, where I has fallen to $(1-2/\pi)$ or about 0.36 times the peak value. The variation of current with $\omega\nu$ is shown in figure 2 for $\frac{2\beta L}{h} = 100$.

The transit time ν is inversely proportional to the velocity and hence varies inversely as the square root of the accelerating potential. Since the range of ν within a peak is small, ν varies approximately linearly with voltage, so that the current also varies nearly linearly with voltage in this small range. If ν is varied in the neighborhood of a peak by variation of the accelerating voltage and if the measured values of current are plotted as a function of voltage, a peak with straight sides will result and the center of the peak can be located quite accurately by interpolation.

The expression used to deduce the above conclusion is not correct for an actual system because of several factors:

1. The electron beam is not of uniform density and does not have a well defined width h.
2. The electrons do not all have precisely the same velocity.
3. The correct equation for displacement includes an initial displacement indicated above by the symbol Δ.

It is difficult to make a complete discussion of these factors until experimental results have been discussed. However, some remarks on the effects to be expected are appropriate here.

If the slit is either narrower or wider than the electron beam

FIGURE 2

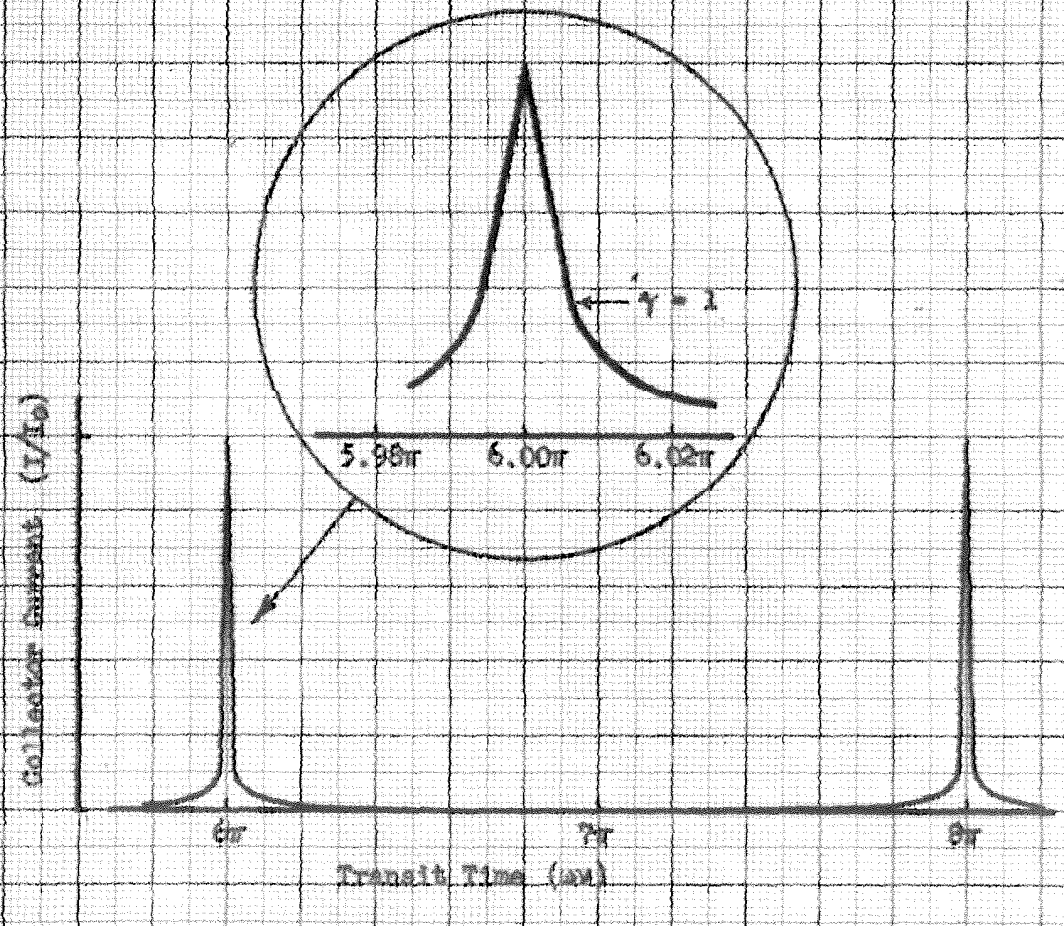

2. Ideal Curve of Collector Current as a Function of Transit Time through Cavity

the peak has a flat top and the sides of the peak are no longer linear, but if the difference in width is small the departure from linearity is negligible. If the beam has unknown density variation the effect is of course unpredictable, but will certainly be small if the variation is small. In all cases, and this is a considerable importance, the peak will be symmetrical whether or not the beam is itself symmetrical.

The effect of a velocity spread of the electron beam has little effect under certain conditions. If for example, the spread in velocity ΔV (expressed in volts) is smaller than the width of the linear portion of one side of the peak (V'), there will still be a region where the curve is linear and has the same slope as the ideal curve. The width of this region will be $(V' - \Delta V)$ and at the edges of this region the curve will slowly depart from linearity in a manner dependent on the particular velocity distribution. The peak will be rounded off for a distance of approximately $\frac{\Delta V}{2}$ on each side of the peak, and the lower limit of the linear portion will be moved inward toward the peak a similar distance. If the width of the peak (expressed in volts) is considerably larger than ΔV, there will be no appreciable effect produced by the velocity distribution.

The effect of the displacement Δ is more important and will be considered in detail later. It is sufficient to remark here that the principle effect is to "round off" the top of the current peak.

IV. SOURCES OF ERROR

Two equations have been given for e/m_o :

$$(4.1) \qquad e/m_o = \frac{c^2 \left\{ \frac{1}{(1 - v^2/c^2)^{1/2}} - 1 \right\}}{V + \Delta V}$$

$$(4.2) \qquad e/m_o = \frac{c^2 \left\{ \frac{1}{(1 - v_2^2/c^2)^{1/2}} - \frac{1}{(1 - v_1^2/c^2)^{1/2}} \right\}}{V_2 - V_1} .$$

In the first of these, the term ΔV is included to indicate that the velocities of the electrons do not correspond to the measured accelerating potential. The value of ΔV is uncertain and cannot be estimated with any accuracy. It includes the potential equivalent to the thermal velocities with which the electrons leave the cathode, work function potentials, thermo-electric potentials, etc.

The first of these is relatively well known. The distribution is Maxwellian and the average values for different temperatures are given in a later section. However, the values for the work function of the materials used are very uncertain and any estimate is apt to be in error by more than a volt. For this reason, equation (4.1) cannot be used to give precise values for (e/m_o) , and equation (4.2) must be used.

Equation (2.18) shows that only three quantities must be measured with accuracy. They are a distance (d) , a frequency (ω) and a difference of potential $(V_2 - V_1)$. A certain probable error in the measurement of either (d) or (ω) results in a probable error in the value of (e/m_o) which is twice as large since both appear raised to the second power.

A probable error in voltage also results in a larger probable error in (e/m_o) both because two readings each subject to error are combined and because the difference $(V_2 - V_1)$ is smaller than the larger of the two voltages.

Errors in the measurement of these quantities can arise in several ways. The distance (d) cannot be taken to be the exact distance between the flat cavity endplates. A correction is necessary because of the finite depth of penetration of current in the cavity walls. In addition a correction may be required because of effects at the holes through which the electron beam enters and leaves the cavity. Thus a probable error in (d) may arise through uncertainties in these corrections as well as through inaccuracies in the actual measurement. A probable error in frequency likewise exists because of uncertainties in the actual measurement and because the frequency can actually vary because the cavities determining frequency have a finite "Q".

The probable error in accelerating voltage has two principal sources, in the actual measurement and in the adjustment of the voltage to the proper value. Factors affecting the latter were mentioned at the end of the preceding section. These factors affect the precision with which the voltage can be adjusted but do not introduce any systematic error requiring a correction.

There is however one additional correction required which is not indicated or implied in equation (4.2) , but which was mentioned in the derivation of this equation. This correction arises because of approximations made in the derivation of the equation and results from the variation in magnetic and electric field because of finite deflection of the beam.

Numerical values for the probable errors cited above will be given

in a later section. An important feature should be pointed out here however. There are only three small corrections to be made, all of which are small enough or can be calculated with sufficient precision to insure small probable error due to these corrections in the value of (e/m_o). Discussion of the effects of these corrections on the precision of the result will also be deferred until later.

V. DESCRIPTION OF APPARATUS

A. RESONANT CAVITY

In the consideration of the theory of this method it was seen that the deflection is proportional to (βL) where $\beta = \frac{e}{mc}\frac{B_{max}}{\omega}$. Relating B_{max}, the maximum value of the magnetic induction, to the power input and cavity constants (see Appendix I) one obtains:

$$(5.1) \qquad \beta = \frac{8e}{mc}\frac{J_1'(0)}{J_1'(ka)}\left(\frac{P}{\omega^3 \Delta a^2 (1+d/a)}\right)^{1/2}$$

where (a) is the radius of the cavity, (d) the length, (Δ) the skin depth and (P) the power input. Since Δ is proportional to $(\omega)^{1/2}$ and (a) to $(\omega)^{-1}$,

$$(5.2) \qquad \beta = K\frac{P^{1/2}}{\omega^{1/4}(1+d/a)^{1/2}} \quad .$$

For reasons explained in a later section, (d) must be kept small compared to (L), but since the length (L) is limited by the maximum permissible physical size of the apparatus, (d) also has a maximum permissible value. Because of this, the ratio (d/a) is found to be less than 1 for usable frequencies. Thus (1+d/a) is approximately 1, and so the deflection varies directly as the square root of the power input and inversely as the 1/4 power of the frequency. Since the deflection is relatively insensitive to change in frequency, the choice of frequency should be governed largely by other considerations such as use of reasonable physical dimensions, ease of obtaining as much high frequency power as possible, suitable transit time with reasonable accelerating voltages.

In the preliminary apparatus it was desired that the electron potentials be large enough to produce well focussed beams with conventional

electron guns and yet small enough so that they could be easily produced, stabilized and measured. In addition, the number of cycles in the transit time could not be too small, or the voltages for successive peaks would differ by so large an amount that separate power supplies would be necessary to investigate each peak. If one sets 1000 volts as the lowest limit on the accelerating voltage, 3 cm. as the maximum value of (d) , and 5 cycles as the smallest number of cycles transit time to correspond to the above values of voltage and distance, the minimum frequency is found to be $\omega = 2n\pi v_o/d \approx 2(10)^{10}$ sec.$^{-1}$ which corresponds to a wavelength of 10 cm. Since a 10 cm. generator was available, this frequency was adopted.

The cavity used was about 12 cm. in diameter and 3 cm. long. It was constructed of brass and had all surfaces silver plated so that a maximum field strength would be obtained from the available power input. To insure proper positioning of the desired mode of oscillation and to minimize undesired modes, narrow slots were cut in the end plates between the regions of maximum electric field. Since the slots were parallel to lines of current flow of the desired mode, the slots did not affect it.

The end plates were accurately machined to make light press fits into the cylinder forming the wall of the cavity. Holes 0.254 cm. in diameter were drilled in the end plates, accurately aligned with the axis of the cavity. These holes were provided to permit passage of the electron beam through the cavity.

When assembled for the final experiments, the measured cavity length was 3.016 cm. and the diameter 12.060 cm. The latter corresponds to a predicted resonant wave length of 9.887 cm. The measured resonant wavelength was also 9.887 cm. A photograph of the cavity and associated equipment is shown in figure 3.

Figure 3

3. Resonant Cavity and Associated Apparatus

B. ELECTRON SOURCE AND COLLIMATOR

The most suitable source of electrons for this work is a hot cathode. In order to make the spread of velocities as small as possible, it is necessary to operate the cathode at the lowest possible temperature. In the following table are given the usual operating temperatures of common electron emitters and the average thermal velocities of the emitted electrons.

Material	Temperature	Ave. Thermal Velocity
Barium Oxide	1000° K	.09 volts
Thoriated Tungsten	1600	.14
Tantalum	2200	.20
Tungsten	2500	.23

The first electron sources to be tried consisted of the electron gun assemblies from commercial cathode ray tubes. These utilized oxide coated cathodes operating at a temperature of about 1000° K. Such cathodes operated satisfactorily for a short time, but soon failed to emit electrons. It is generally believed that the operation of such cathodes depends on the presence of small amounts of metallic barium produced from barium oxide by reducing action during activation. During operation, any oxygen present will combine with barium to again form barium oxide. If additional reducer is present, the supply of metallic barium can be maintained for a short time, but eventual failure is to be expected. This hypothesis seems to explain the failure of such cathodes in the present apparatus. The pressure in the vacuum system was approximately 10^{-5} mm. of mercury. The gas present contained oxygen and there seemed to be no very satisfactory way to eliminate it to the extent necessary.

Some consideration was given to the use of thoriated tungsten,

tantalum and pure tungsten. The latter was chosen for initial tests because of its greater ability to withstand positive ion bombardment and because it was readily available in a form suitable for filaments. Other materials were to be investigated if the electron thermal velocities for tungsten filaments had a noticeable effect on the performance of the apparatus. The filaments were made of tungsten wire .006" in diameter wound in a three turn helix about .020" in diameter. The filament was spot welded to two nickel wires which served both as supports for the filament and conductors for the heating current. The filament assembly was inserted into an electron gun from a standard cathode ray tube, with the middle turn of the helix directly behind the hole in the first grid. Such a filament produced an electron beam with an intensity of a few microamperes for heating currents of about 2.8 amperes.

The beam produced by the electron gun, while reasonably well focussed by ordinary standards was by no means sufficiently parallel for the present apparatus, and a collimator was necessary to select a satisfactory portion of the beam. The arrangement was typical and is shown schematically in Figure 4. Two pairs of deflecting plates at right angles to each other were provided following the first two slits in order to permit lateral adjustment of the beam. All slits could be opened by levers operating through vacuum tight flexible metal diaphragms. Rotary adjustment of the third slit was made possible although it was later evident that this adjustment was unnecessary for reasons to be discussed later.

The "collector" was mounted in a Faraday cage behind the third slit. The collector was maintained at a positive potential with respect to the slit and shield so that secondary electron would not escape. A potential of 20 volts was sufficient to collect virtually

FIGURE 4

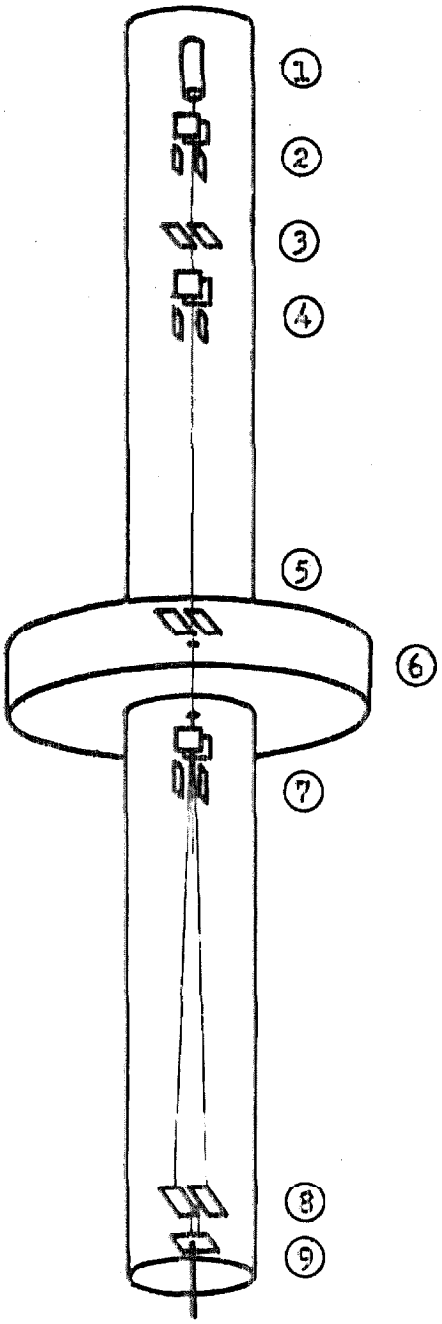

1. Electron Source
2. No. 1 Deflection Electrodes
3. No. 1 Slit
4. No. 2 Deflection Electrodes
5. No. 2 Slit
6. Resonant Cavity
7. No. 3 Deflection Electrodes
8. No. 3 Slit
9. Collector

4. Schematic Diagram of Collimating and Detection System

all of the secondaries.

As mentioned earlier, the total beam current was approximately one microampere. However that portion selected by the collimator was less than one hundredth as large so that a meter with a maximum sensitivity of about 10^{-9} ampere for full scale deflection was required. The circuit diagram of the meter used is shown in Figure 5.

C. POWER SUPPLY FOR ELECTRON GUN

The power supply for the electron gun was conventional in design except that ordinary vacuum tubes were used under somewhat unusual operating conditions. The tubes were used with plate voltages ranging from 500 to 2000 volts although the plate currents were kept sufficiently low so that allowable plate dissipations were not exceeded. Tubes of the "7N" series were used to eliminate the possibility of dielectric breakdown at the tube base. The basic regulator tube was a low mu tube, and the amplifier tube a high mu tube. The voltage standard for the circuit was a 400volt dry cell battery which was inserted in the grid circuit of the amplifier tube so that the battery current was essentially zero.

The output voltage could be adjusted between the limits of approximately 600 and 2000 volts. The ripple content was less than 1 part in 50,000 at all output voltages and the output voltage varied a negligible amount for ordinary changes in line voltage. The circuit is shown in Figure 6.

D. HIGH FREQUENCY ELECTRICAL SYSTEM

A schematic diagram of the high frequency system is shown in Figure 7. The generator was a double ended klystron with a plate voltage rating of 2000 volts and plate current rating of 50 mils.

FIGURE 5

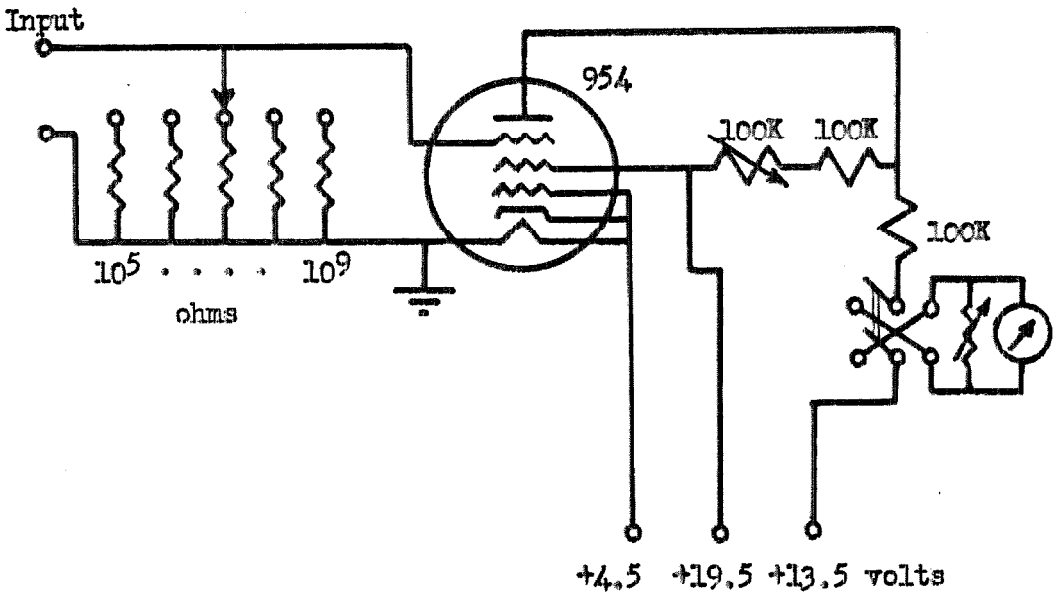

Maximum Sensitivity : 0.5 μ ampere per $(10)^{-11}$ ampere

5. Circuit Diagram of Meter for Measuring Collector Current

FIGURE 6

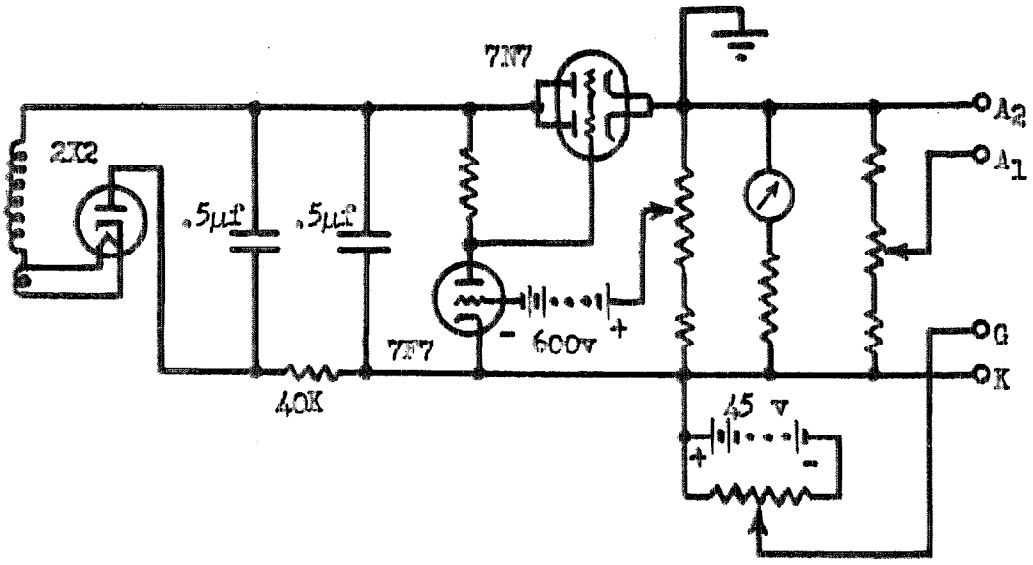

6. Regulated High Voltage Power Supply

FIGURE 7

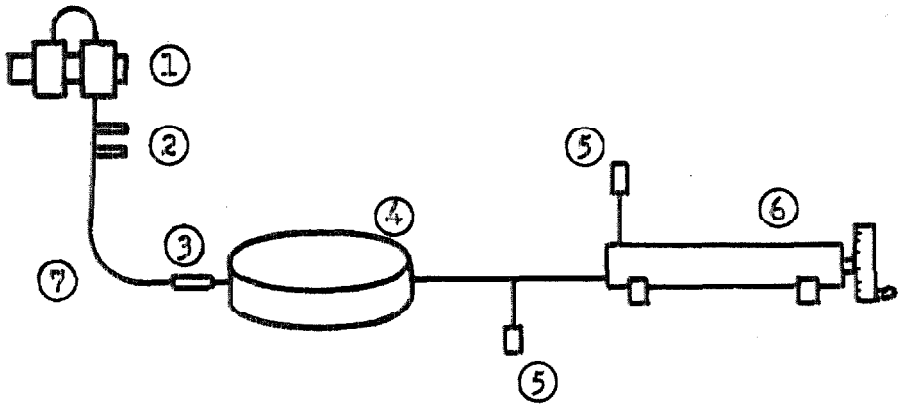

1. Klystron
2. Double Stub Tuner
3. Line Stretcher
4. Cavity
5. Detectors
6. Frequency Meter
7. Coaxial Line

7. Schematic Diagram of High Frequency Electrical System

It was found that it could deliver a few watts into a properly matched load. Ordinary 50 ohm coaxial cable was used for transmission of the power. A "line stretcher" and two tuning stubs 3/4 wavelength apart were provided to insure a suitable impedance match and hence maximum transfer of power. However, it was found that when the coupling loop in the cavity was adjusted in area to produce an input impedance of about 50 ohms, the matching elements were quite unnecessary. For measurement of field strength and frequency, a small amount of the cavity power was taken by a very small coupling loop and measured by conventional detectors and a frequency meter of the coaxial cavity type. As noted above, the apparatus could deliver a few watts into the cavity producing field strengths of the order of 500 volts per cm. and 2 Gauss.

E. VACUUM SYSTEM

A relatively simple vacuum system was used for this work. The basic apparatus was constructed of brass. All joints were either soldered or coated with beeswax-resin mixture to make them vacuum tight. Where mechanical motion was necessary, sylphons and thin metal diaphragms were used.

The pumping system consisted of a Hyvac mechanical fore-pump, a reservoir, two stage mercury diffusion pump, liquid air trap, and ionization gauge for pressure measurements. The connection between the glass pumping system and the metal apparatus was achieved by use of a tapered glass to metal seal which was sealed with wax.

Since outgassing of the metal parts was impossible, a "high vacuum" could not be achieved. However, it was usually possible to obtain pressures between $^{1}/_{2}$ and $2(10^{-5})$ mm. of mercury at the ionization gauge. This was believed adequate for the purpose, since the

only requirement was that the mean free path of the electrons be somewhat greater than the length of the collimating tube.

VI. OPERATION OF APPARATUS

A. ADJUSTMENT

The electron beam was capable of being measurably affected by the relatively small magnetic field within the resonant cavity and was therefore very sensitive to stray fields. In fact periodic fields of only .005 volts per cm. and .0005 Gauss were sufficiently large to reduce the precision of the experiment. To eliminate electric fields it was sufficient to surround the apparatus with a metal shield. Magnetic shields are not so readily constructed, so the effects of magnetic fields were eliminated in other ways.

A static magnetic field such as the earth's field does not affect the functioning of the apparatus provided satisfactory collimation of the beam can be achieved. However, unless the electron beam is approximately aligned with the earth's field, the magnetostatic deflections are too large to permit proper collimation at all accelerating potentials. Such alignment did not however eliminate all of the undesirable effects of the earth's field. The electrons produced by the usual electron gun do not move in accurately parallel paths. The collimating slits produce a beam which is narrow in one direction, but wide and diverging in the perpendicular direction. Due to this divergence the axial magnetic field of the earth has a defocussing action. If the electrons were diverging from a point, the effect would be to merely rotate the beam, producing an image of one slit rotated at the next slit. For the electron velocities used in this experiment, the rotation amounted to approximately 10° per meter distance. If the divergence was not from a point, then there would be in addition a broadening of the image of the slit. With the apparatus described, the first effect was found to be much greater than the latter.

To eliminate the effects, the axial component of the earth's field was neutralized by passing an electric current through a solenoid wound uniformly over the entire length of the tubes forming the collimating and drift regions.

This compensating coil was found useful for another reason. Adjustment for parallel alignment of the slits was made by eye and could not be made with great accuracy. Since small axial magnetic fields produced small rotations of the beam without detectable broadening, the beam could be made to coincide in alignment with a slit by adjustment of the current in the solenoid. This adjustment was of course not necessary when making measurements by visual observation of the beam, but it was used when making adjustments for taking data by measurement of the collector current.

The effect of periodic magnetic fields was eliminated by removing all sources of appreciable magnetic field. Many sources which might not be suspected of disturbing the beam were actually troublesome since a field of .0005 Gauss was sufficient to produce a disturbing effect. For example, the current in the diffusion pump heaters produced a field in excess of .01 Gauss even at a distance of 3 meters, so that direct current had to be used in these heaters. An unusual source of field was found in connection with the use of mercury pumps. The phenomenon of flashing in mercury pumps was observed. It was found that the flashover was accompanied by a flow of current sufficiently large to disturb the beam. The effect was minimized by moving the pumps as far as feasible from the apparatus (approximately 10 meters), and shielding the pumps with transformer iron.

The transformers in the power supplies for the electron gun and klystron likewise produced appreciable fields. The power supply for the latter was merely moved to a great distance (approximately 10 meters),

However, since the power supply for the electron gun had to be located nearby for ease of control of voltage, the transformers for this apparatus were provided with "mu-metal" and copper shields which reduced the fields by approximately 40 db (a factor of 100). The last troublesome periodic field was finally found to arise from a small 1/4 horsepower electric motor operating on a lower floor of the building.

B. OPERATING PROCEDURE

The first experiments with the apparatus were intended to demonstrate that it behaved qualitatively as the theory indicated. The first test relating to the precision of the method was to determine the accuracy with which the accelerating voltage could be adjusted. This was first done by visual observation of a fluorescent screen placed in the path of the beam at the end of the drift tube. The maximum deflection of the beam was observed to be approximately 2 mm. to either side of the center position. Since the drift distance was 1 meter, this indicated a field strength within the cavity of approximately 2 Gauss. Assuming a reasonable value for the skin depth of the cavity walls, a calculated power input of two watts was obtained.

Adjustment of the voltage was made as shown in Figure 8. The control on the power supply was set to approximately the desired value, and an additional potentiometer was used to add a small adjustable and accurately measurable voltage to the well stabilized power supply voltage. Several values of the incremental voltage were obtained at the peaks corresponding to $n = 4$ cycles and $n = 5$ cycles by repeatedly setting the potentiometer voltage away from the proper value and approaching it alternately from opposite directions. The consistency of the results indicated that the voltage could be set with a probable error of about 1 volt. Some of the data are shown below:

FIGURE 8

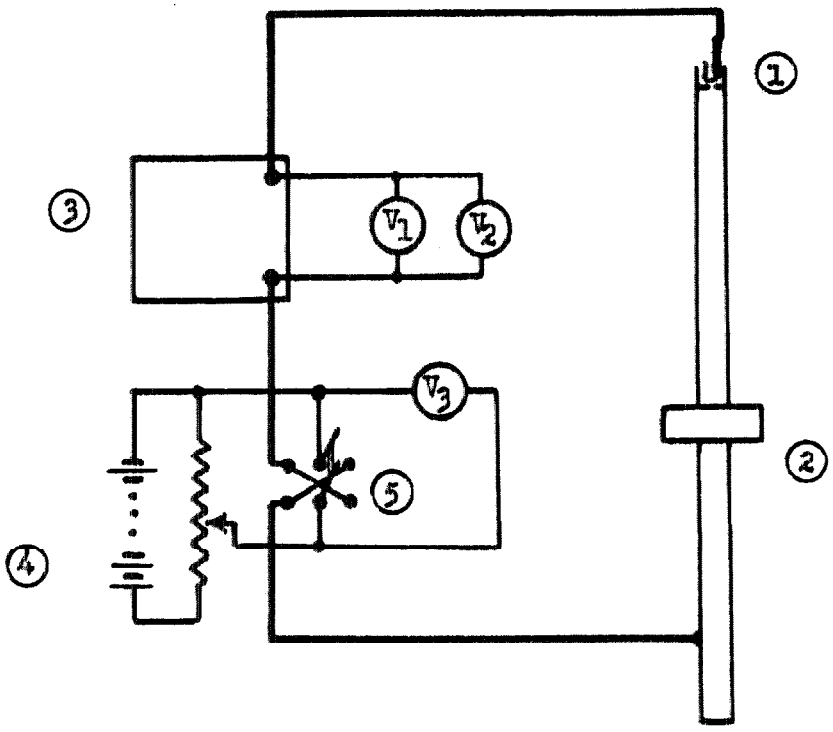

1. Electron Source
2. Apparatus Shield
3. Power Supply (500-2000 volts)
4. Battery (45 volts)
5. Reversing Switch

V_1 Electrostatic Voltmeter

V_2 Low-current Voltmeter

V_3 Voltmeter (0-50 volts)

8. Circuit for Adjustment and Measurement of Accelerating Voltage

Incremental Voltage for Null Deflection

Visual Observation of Beam

	Approached from below	Approached from above
	$18^{1}/_{2}$ volts	17 volts
	16	17
	20	18
	17	19
Mean	18	17.8

The second set of tests involved measurements of beam current in the manner described in section III. Considerable difficulty was encountered in obtaining consistent readings. Three sources of trouble were encountered, although they were all ultimately traceable to one basic cause, namely the effect of stray magnetic fields. The least troublesome was the fact that the earth's field was by no means uniform in the room in which the apparatus had been set up, and hence the alignment of the apparatus with the earth's field was at best an approximation. Consequently the electron trajectories in the absence of cavity excitation were not straight lines. As a result, the accelerating potential influenced the trajectory, and the position of the electron beam at the end of the drift tube varied slightly as the potential was varied. This of course shifted the beam from the slit, and readjustments had to be made as the potential was varied.

Random motion of the beam was also observed. This seemed to be largely due to the fields produced by the vacuum pumps. Shielding of the pumps, and removing them to the greatest practicable distance reduced the effect but did not eliminate it principally because the iron used for shielding was not of sufficiently high permeability. Such deflections of the beam in the collimating system resulted in random

variations in total beam current, while such deflections in the drift space caused variations in the proportion of the current passing through the slit. By taking nearly simultaneous readings of the collector current with cavity power on and off, consistent readings could be obtained. Some of the data taken are shown in Figure 9.

A few remarks regarding these data are necessary. The three slits were made .005", .003", and .007" in width in that order. Since the distances between slits were approximately equal, the maximum expected beam width at the third slit was (.005 + 2(.003)) = .011". It was found that the observed width was approximately this value since 65 percent of the total beam current passed through the .007" slit.

When making readings, the width of the third slit was increased to allow about ninety percent of the total current to pass through the slit when there was no field in the cavity. If the maximum deflection is known, the slopes of the sides of the peaks can be calculated using equations (3.2) and (2.12). No accurate measurement of the maximum deflection was made, but based on an estimate of this deflection, the computed value of this slope was .02 volt^{-1}, this is somewhat larger than the measured value of about .012 volt^{-1}, but due to the uncertainty in the values for the beam width and the maximum deflection, the agreement is perhaps satisfactory.

The linearity of the curves drawn from the experimental data is remarkable. Close examination of the "fit" of the points to the curve of Figure 9 indicates that the intersection of the two lines can be taken to be the center of the peak with a probable error certainly less than $^1/_2$ volt. In any case the accuracy is probably greater than can be achieved by visual observation of the beam, and subjective factors

FIGURE 9

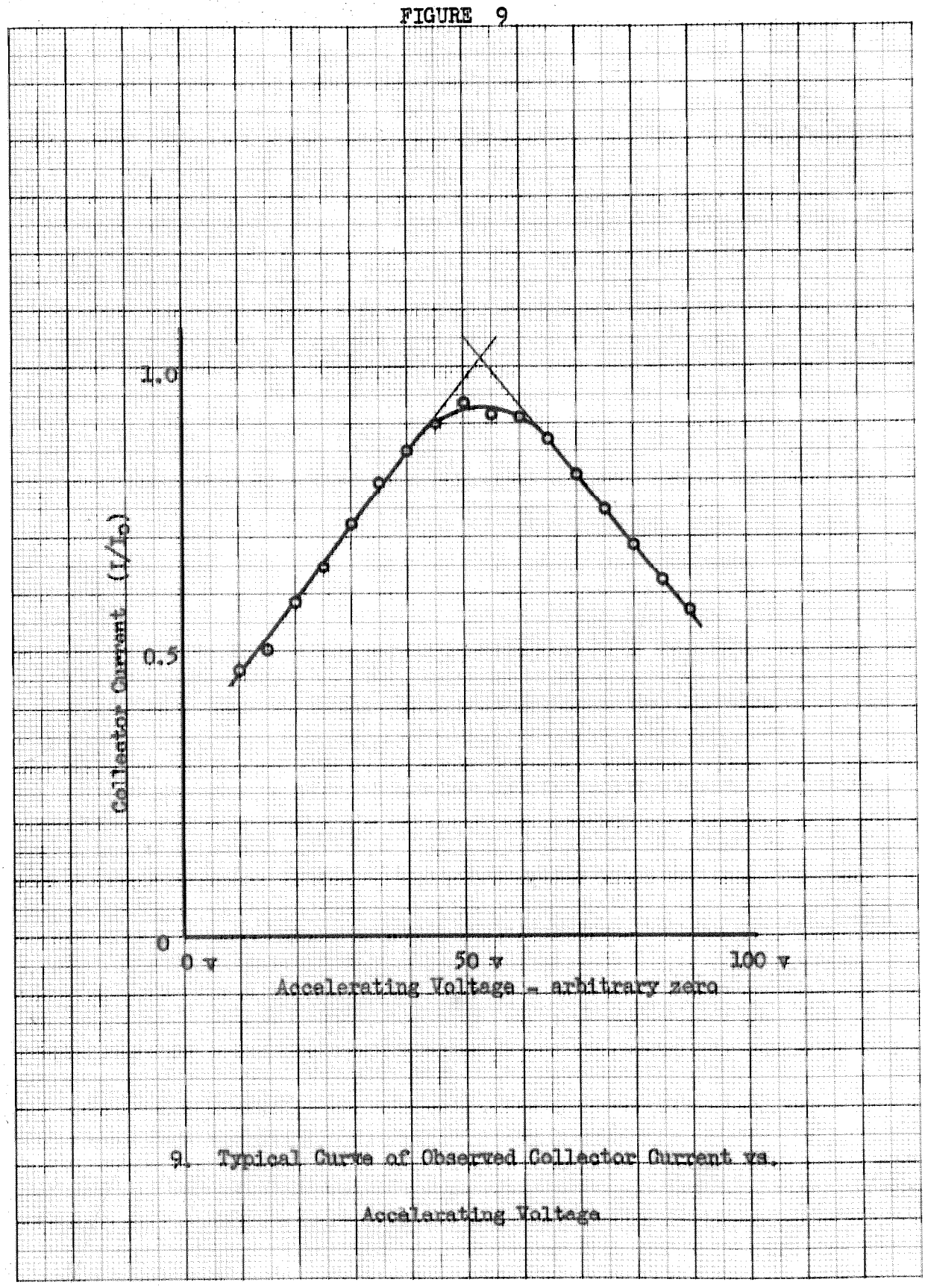

9. Typical Curve of Observed Collector Current vs. Accelarating Voltage

in setting the accelerating voltage are eliminated.

The third set of tests was made to obtain an approximate numerical value for e/m_o . All necessary quantities were either known or had been measured except the accelerating voltages which gave no spread of the beam when the cavity was excited. Since the experiments were largely exploratory in nature, a complex setup for measurement of voltage was not thought justifiable and simple voltmeters were used for this measurement. The power supply for the electron gun could supply only a few mils of current, so that ordinary precision voltmeters with 10 mil movements could not be used. However a meter with a low current (300 microamperes) movement and an electrostatic voltmeter were obtained and carefully calibrated against standard voltmeters throughout the range from 600 to 2000 volts. These meters were used with the circuit of Figure 8 as explained earlier. This arrangement permitted variation of the voltage V_1 and readjustment of the incremental voltage V_2, thus eliminating systematic errors in reading the meters.

The adjustable power supply was set to a voltage near the proper value and the potentiometer was adjusted visually to the proper value. The two high voltage meters were read, corrections applied, the two values averaged, and the potentiometer voltage added, giving the accelerating voltage except for the constant correction ΔV of section IV. By adjusting the power supply to a slightly different voltage and repeating this procedure another value for the accelerating voltage could be obtained and used to check the accuracy with which the voltage could be read. It was first estimated that the corrected mean for the higher voltage could be obtained with a probable error of about 5 volts. However, the readings taken in this manner all agreed within one volt! This surprising consistency held even for readings taken on successive

nights. Certainly this is partly coincidental, although it is not surprising that the voltage readings are more consistent than would be expected from a pessimistically estimated probable error.

VII RESULTS

For comparison of experimental and expected results, it is more convenient to compare the observed and expected values of accelerating voltage rather than calculated values with expected values of e/m_o. The values for the expected voltages were computed from equations (2.1) and (2.15) using the accepted value of e/m_o (5). Voltages were measured for the number of cycles in the transit time equal to 4 and 5. The data obtained are given below:

Number of Cycles	Accelerating Voltage	
n	Expected	Observed
4	1477	1492
5	944.5	954
difference	532.5	538

The difference between expected and observed values was certainly larger than the errors in reading the voltage, much larger than any thermal emf, contact potentials, or potentials equivalent to the thermal velocities of the electrons. Furthermore, the difference was too large to be ascribable to errors in measurement of frequency or cavity length. It is certainly significant that the observed values differed from the expected values by a nearly constant percentage, 1 percent. This implied an unforseen systematic error.

Re-examination of the equations revealed a possible explanation. The derivation given earlier assumed a magnetic field which was uniform over a given length, but which had perfectly sharp boundaries outside of which the field was zero. This assumption is quite valid where the metal surface of the cavity forms the boundary, for the "skin depth" of the metal is very small compared to the length of the cavity. However, at the small holes where the electron beam enters and leaves the cavity, the field is disturbed and there is a "fringing" of the field

which might alter the effective length of the cavity.

The analysis of this effect is straightforward and is given in Appendix III. If one considers a magnetic field which has a maximum value ($\bar{B}_m$) throughout most of the interval of length (d), has a value ($\bar{B}_m/2$) at the end points of the interval and rises from 0 to ($\bar{B}_m$) symmetrically about the value ($\bar{B}_m/2$), then there is no correction whatever to apply to the equation derived for (e/m_o), but in equation (2.7) for the lateral velocity, ($\dot{x}$), a factor which differs very slightly from 1 must be inserted.

If the boundary is not symmetrical in the sense given above, the conclusion is only approximately valid, but one can determine whether the distance (d) should be increased or decreased by investigating the precise nature of the field near the boundary. This investigation can be made quite accurately by consideration of a problem in magnetostatics, because the dimensions of the region of disturbance are very small compared to the wavelength of the oscillation. The problem is then to find the solution for the equation $\nabla^2 V = 0$ where the field lines are uniform and parallel at a great distance from the origin. The proper boundary condition to apply in this case is that the field lines are parallel to the surface of the metal forming the cavity wall and the entry or exit hole.

The cavity had been constructed approximately as shown in Figure (10a). Unfortunately the numerical solution of the problem above with this boundary condition is very difficult. However, three cases which can be readily solved were considered. These were (1) penetration of magnetic field into a slit in an infinite sheet, (2) penetration into an infinitely deep slot in an infinite plane, and (3) penetration into a circular hole in an infinite sheet. These various boundary conditions

FIGURE 10

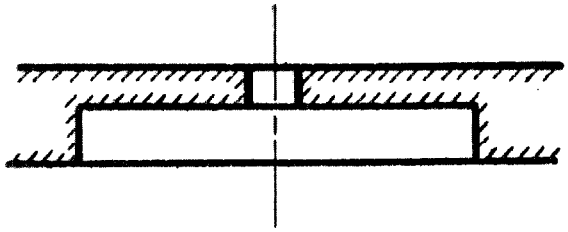

(10a) Initial Shape of Cavity End Plates

(10b) Hole or Slit in an Infinite Sheet

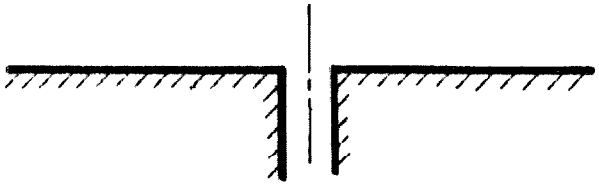

(10c) Slot of Infinite Length and Depth

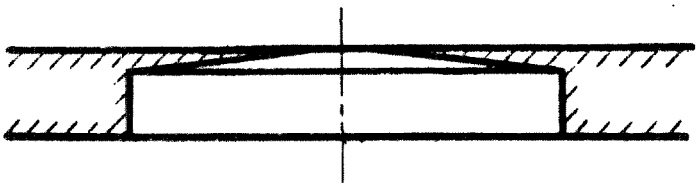

(10d) Final Shape of Cavity End Plates

10. Actual and Ideal Boundary Conditions at Entry and Exit Holes of Resonant Cavity

are illustrated in Figures (10b) and (10c). The solutions of these problems are given in Appendix IV, and plots of the resulting fields on the axis of symmetry are given in Figure (11). For cases (1) and (3) above the field is precisely symmetrical with respect to the sheet (in the manner described above) not only on the axis, but at all points. In these cases, therefore, the correction to be applied is certainly zero. For case (2) above the field is not precisely symmetrical, but nearly so. However, the midpoint of symmetry is not at the surface of the slit, but below the surface a distance approximately equal to five percent of the slit width.

Consideration of the problems above leads one to feel intuitively that the effect for the actual problem is intermediate between that for cases (1) and (3), and case (2). One might therefore expect to find the "effective length" of the cavity slightly larger than its true length. Examination of equation (2.18) shows that the cavity length inferred from the experimental results is larger than the measured value by $^1/_2$ percent. This corresponds to a correction equal to about 3 percent of the diameter of the hole. This result is entirely consistent with the discussion above.

Rather than attempt to solve the difficult potential problem of Figure (10a), the cavity end plates were re-shaped to conform as nearly as possible to the problem which could be solved rigorously. This was done as shown in Figure (10d). The half angle of the conical surface was made nearly equal to 90 degrees (approximately 85 degrees). Using these end plates, new measurements were made. The results are given as following:

FIGURE 11

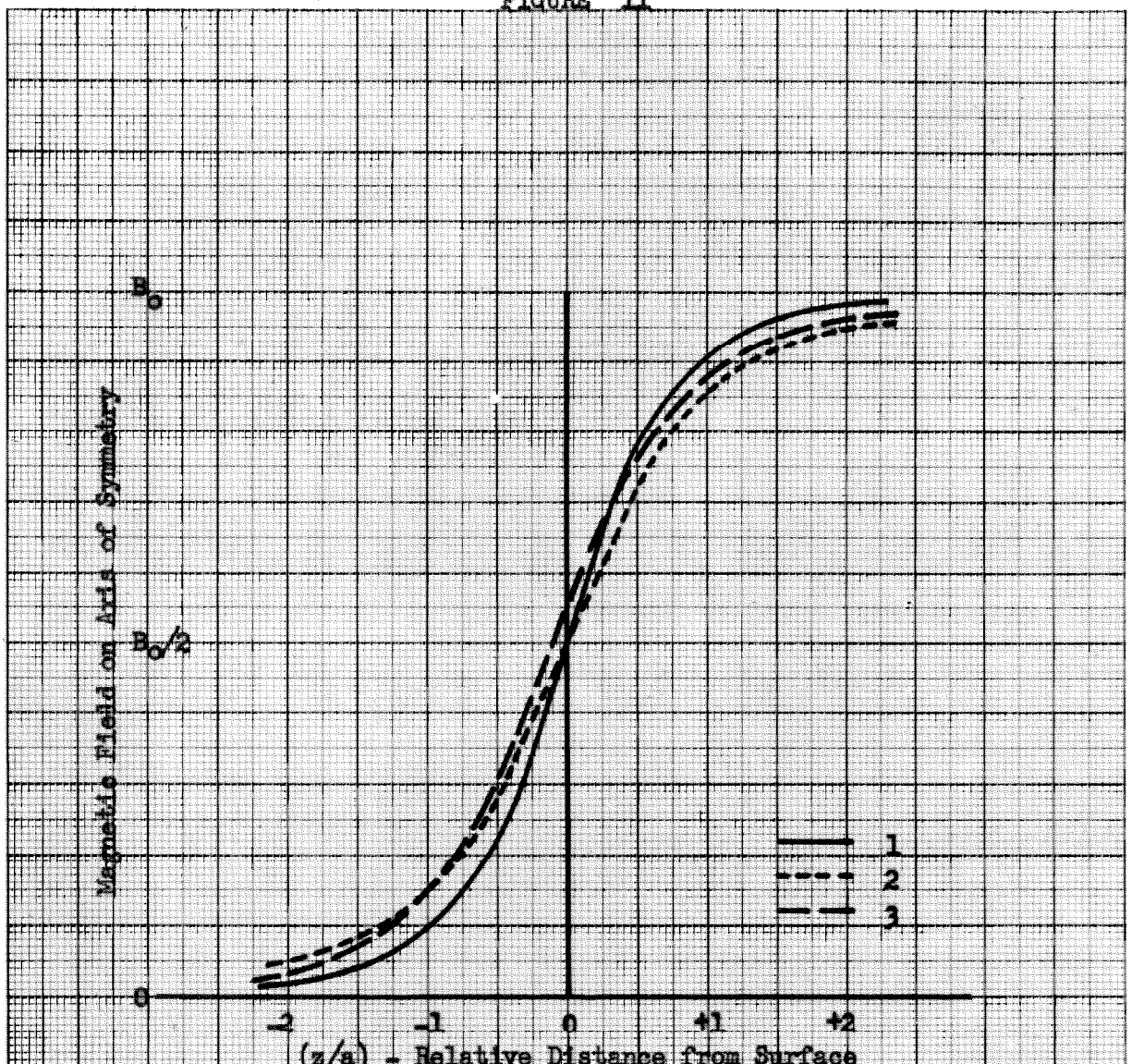

1. Hole of radius (a) in an infinite sheet

2. Slit of width (2a) in an infinite sheet

3. Infinitely deep slot of width (2a)

11. Magnetic Field on Axis for Various Boundary Discontinuities

Number of Cycles	Accelerating Voltage	
n	Observed	Expected
4	$1494^{1}/_{2}$	1497.1
5	954	956.5
Difference	$540^{1}/_{2}$	540.6

The internal consistency of the two sets of data and the good agreement in the second set with the expected value indicate that the cause of the discrepancy had been eliminated.

VIII PRECISION OF RESULT

The frequency (ω) was determined in two ways, by measurement of the physical dimensions of the cavity and calculation of the resonant frequency, and by use of a coaxial type wavemeter to measure the frequency when the cavity was actually excited. In the first method, a diameter of approximately 5" was measured with calibrated micrometers, the apparent probable error being about .0005", or about 1 part in 10,000. In the second method, the meter could be read and consistently set to the proper value with a probable error also of 1 part in 10,000. The two values fortunately agreed to this precision, both values being equivalent to a wavelength of 9.887 cm. .

The distance (d) was measured by carefully measuring the component parts of the cavity and calculating the internal spacing. The probable error in this measurement was estimated to be approximately 5 parts in 10,000, and hence the probable error in (d^2), 1 part in 1000. The "skin depth" of the cavity wall was about 10^{-4} cm. and hence involved negligible correction. It is believed that the end effects discussed earlier are much smaller for the final end plates than the probable error in measurement.

The measurement of voltage is probably the most critical and most difficult. As mentioned earlier, it is believed that the potential was measured in spite of the relatively crude instruments with a probable error much smaller than first seemed reasonable. This belief is reinforced by the fact that sucessive readings taken in such a way that one could not possible influence the next all agreed within $\frac{1}{2}$ volt. However, allowing for inevitable errors in calibration of meters, it seems reasonable to set the probable error in voltage measurement at 1 $\frac{1}{2}$ volts.

The voltage difference (V_2-V_1) was approximately 500 volts. This therefore represents a probable error in (V_2-V_1) of two volts or about 4 parts in 1000.

Since the probable error of measurement of frequency and distance was small compared to the one discussed above, the probable error in the result is dependent almost entirely on the probable error in measurement of voltage. The resulting calculated value for (e/m_0) thus has a probable error of about 4 parts in 1000. The value obtained was

$$e/m_0 = 1.759 \pm .007 \quad (10)^7 \text{ abcoulombs per gram.}$$

This is remarkably close to the presently accepted value (5)

$$e/m_0 = 1.7592 \pm .0005 \quad (10)^7 \text{ abcoulombs per gram.}$$

IX. PRECISION ATTAINABLE

The apparatus could be used with essentially no major changes to yield data of somewhat higher precision. If voltage measuring apparatus were provided which could be used to measure the voltage to a greater precision than that with which it could be set, the only significant error in voltage measurement would be in adjustment of the accelerating voltage to the proper value, which would result in a probable error for $(V_2 - V_1)$ of about 1 part in 1000. Combining this probable error with that in cavity length, (d), the probable error in (e/m_o) would be about $1\ ^1/_2$ parts in 1000.

In view of the precision of the most recent determination of (e/m_o)[2] it is apparent that the precision of measurement by this method must be increased by a factor of about 10.

The principal factors which influence the precision are:

1. Cavity frequency (ω)
   - (a) Uncertainty in frequency
   - (b) Measurement of frequency
2. Cavity length (d)
   - (a) Measurement of distance
   - (b) Correction for "skin depth"
   - (c) Fringing effect at entry and exit holes
3. Accelerating voltage $(V_2 - V_1)$
   - (a) Adjustment of voltage
   - (b) Measurement of voltage
   - (c) Velocity distribution of electron beam
4. Approximations in derivation of electron trajectories.

Systematic discussion of these factors is rendered difficult by the fact that a given change in the apparatus or technique to reduce the probable error due to one of these factors may increase the probable error due to another. Anticipating the final result, it may be remarked in advance that a probable error in the final result of about 1 part in 10,000 seems possible. Consequently any quantity which can be measured with a probable error of a few parts in 100,000 will have little effect in determining the total probable error.

(1) Cavity frequency: The cavity determining the frequency in this apparatus has a "Q" of approximately 30,000, so that the operating frequency is determinable with a probable error substantially smaller than $^1/_2$ part in 10,000 affecting the precision of the result to an extent correspondingly less than 1 part in 10,000. On the other hand, in order to conveniently measure the frequency it may be desirable to use a lower frequency generator whose frequency can be more readily measured and which can be stabilized with even greater precision, the operating frequency being obtained by frequency multiplication. It appears possible to establish and measure the frequency with a probable error much less than $^1/_2$ part in 10,000.

(2a) Measurement of cavity length: Measurement of distance with the desired precision cannot be made with conventional measuring tools such as micrometers. However, optical methods afford satisfactory ways of making this measurement so that the precision of the result would not be affected by errors in this measurement.

(2b) Skin depth correction: At the frequency used, the skin depth for silver is about $(10)^{-4}$ cm., so that for a cavity length of 3 cm.,

a correction for skin depth amounts to less than 1 part in 10,000 of the cavity length, thus affecting the result to the extent of nearly 2 parts in 10,000. The probable error introduced by the correction should be somewhat smaller than this.

(2c) Fringing effect at entry and exit hole: In the discussion of this effect in section VII it was shown that this effect can be calculated and also that it can be made zero with certain ideal configurations which can be approximately achieved in practice. However such an approximate realization (see Figure 10d) renders accurate knowledge of the distance between surfaces (d) more difficult because of possible warping near the hole. Use of entry and exit holes of a different nature such as shown in Figure (10a) requires calculation of the end effect, which is certainly not zero in this case, even though the distance (d) can then be determined with a greater precision. Furthermore, since the electron beam is not concentrated at the precise center of the hole, the end correction may vary for different portions of the beam.

A practical solution may be to use end plates of the type shown in Figure (10d) where the end correction is known to be substantially zero, but where a relatively large probable error in (d) exists. If the same end plates are then used with a cavity of different length, the proper correction to give consistent values can be computed. An alternative solution may be to use end plates of the type shown in Figure (10a) where the end correction must be calculated. If the electron beam can be confined to a sufficiently small region radially, the correction will be substantially the same for all portions of the beam.

Any attempt to reduce the effect of the above probable errors by increasing the length of the cavity will reduce the precision with

which the accelerating voltage can be determined. This will be discussed later.

(3b) Measurement of voltage: Discussion of methods of measurement of voltage is not within the scope of this paper. It is sufficient to remark that use of a suitable potentiometer and standard cells permits accuracy far in excess of that required.

(3c) Effect of distribution of electron velocities: The effect of the distribution of velocities decreases as the accelerating voltage is raised. At the value recommended below, the center of the collector current peak must be located with a probable error of about 0.15 volts, so that the peak should have a width of 10 or 15 volts. In such a case a spread of velocities equivalent to about 0.3 volts will not affect the shape of the collector current curve except in the neighborhood of the top where it will be more seriously modified by other factors mentioned below. The conclusion is that the velocity distribution in an electron beam from a tungsten filament should have no effect on the precision of the method.

(3a) Adjustment of voltage: With the transit times used for the measurements described in section VII, the two values for accelerating voltage were approximately (950) volts and (1500) volts, and the difference was approximately (550) volts. An improvement in the data would apparently result if the value of (V_2-V_1) could be increased relative to (V_2). The accompanying table gives the approximate values of the accelerating potential for various values of the integer (n) (the number of cycles of the cavity oscillation during the transit of an electron through the cavity).

n	1	2	3	4	5	6
V (volts)	26,000	6,000	2,650	1,500	950	660

The most practicable value for the larger value of (n) seems to be $n_1 = 5$, so that (V_1) is equal to about 950 volts. If now (n_2) is made equal to 1 or 2 so that (V_2) is very large compared to (V_1), the probable error in (V_2-V_1) should be essentially equal to the probable error in measurement of (V_2) alone. However, such a value of (n_2) does not give the minimum probable error. This is due to the fact that the experimental procedure gives rise to a certain probable error in $(\omega\nu)$ rather than in (V). Since $(\omega\nu)$ varies inversely as the square root of the voltage, the percentage probable error in (V_2-V_1) actually has its minimum value for $n_2=3$. For this case, the larger accelerating voltage (V_2) has a value of (2700) volts.

If a probable error of 1 part in 10,000 is to be achieved, this larger voltage must be adjusted to the proper value with a probable error of about 0.15 volts. This requires a resolving power in the apparatus equivalent to a probable error of 0.07 volts for $n_2=4$ which is the value that was actually used in the earlier experiments. Since the apparatus gave results with a probable error of about 0.5 volt for this value of (n_2), it is necessary to increase the resolving power by a factor of only 7 to achieve the desired accuracy.

Investigation of the possibility of achieving this requires reconsideration of the deflection equation, and a short digression on item (4) of the table opening this section.

(4) Approximations in derivation of electron trajectories: In section II, where the theory of this method was presented, exact integration of the equations of motion for an electron could only be achieved if the magnetic field were taken to be uniform throughout

Figure 12

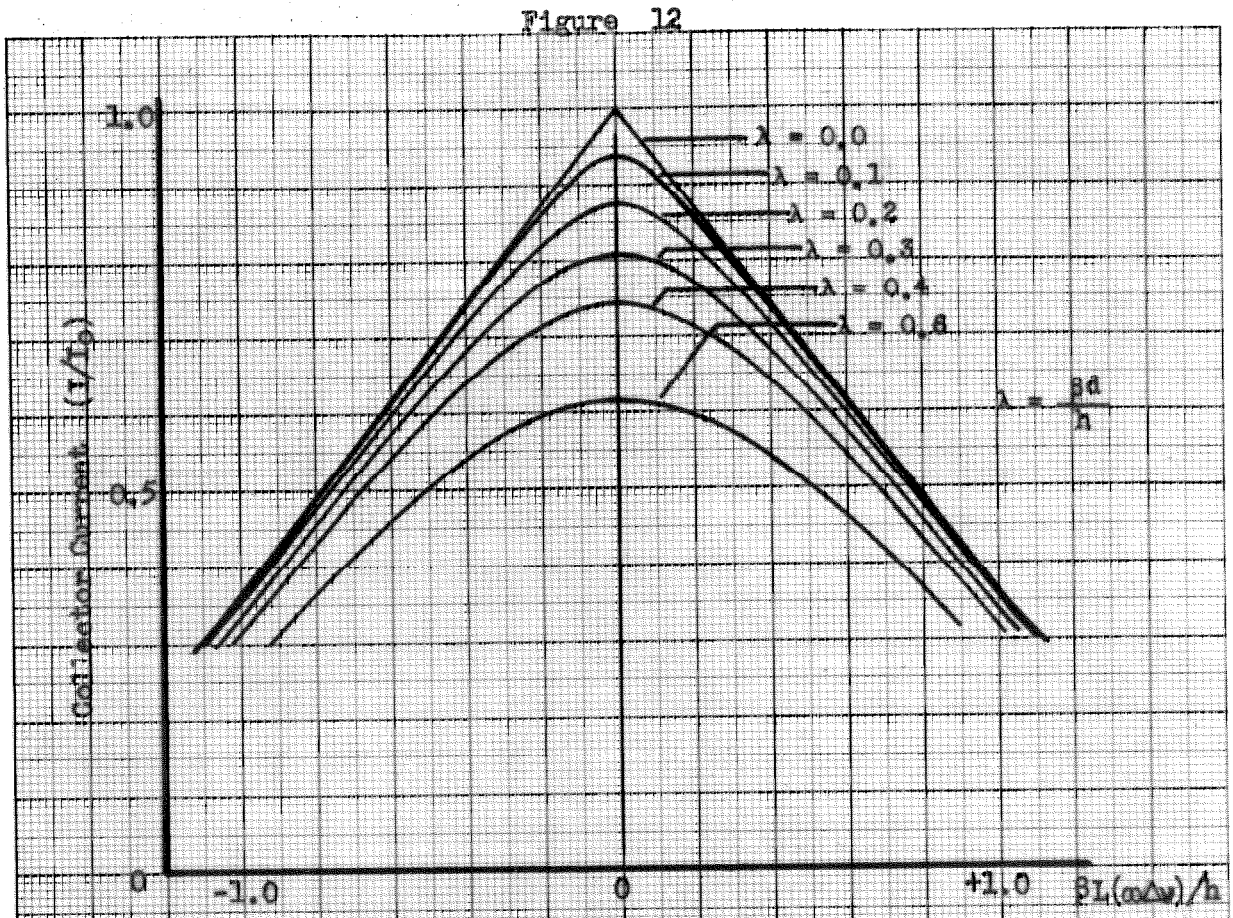

(12a) Theoretical Collector Current Curves

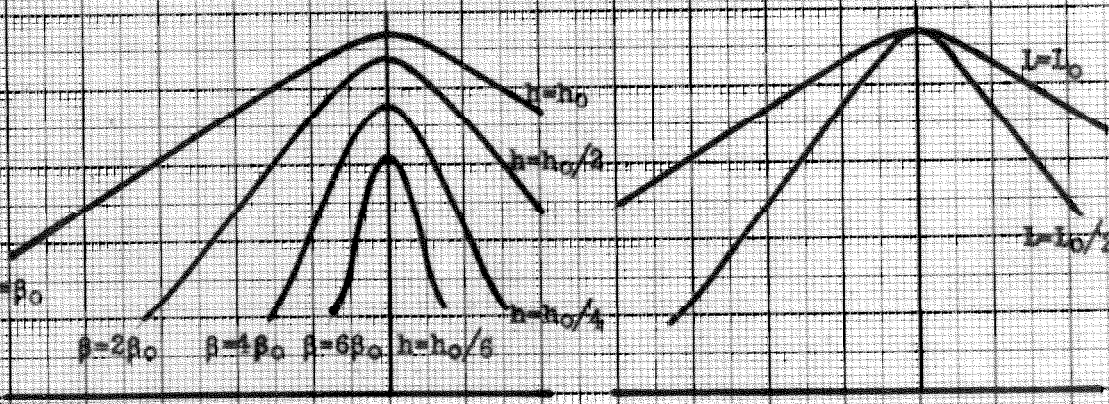

(12b) Effect of Increase of Field Strength or Decrease of (h)

(12a) Effect of Increase of Drift Length (L)

12. Theoretical Collector Current Curves for Various Conditions of Operation

the region of motion of the electron. Actually if the electron suffers a finite deflection from the Z axis, the magnetic field decreases slightly and a small electric field appears. More correct equations of motion are:

$$\ddot{x} = \beta\omega\dot{z}(B/B_0)\cos\omega t \tag{9.1}$$

$$\ddot{z} = -\beta\omega\dot{x}(B/B_0)\cos\omega t - eE_z = -\beta\omega\dot{x}(B/B_0)\cos\omega t + \beta\omega^2 x\sin\omega t \tag{9.2}$$

where $(B/B_0) = (1-3k^2x^2/8)$ (see Appendix I),

and the other notation is that of section II.

Solutions of these equations can be obtained most readily by successive approximations. The results contain complicated combinations of trigonometric functions which are defficult to interpret. Fortunately most of these terms are multiplied by coefficients which are very small compared to the terms considered in section II so that they can be safely ignored if a probable error of about 1 part in 10,000 is being considered. The principal effect is observed in the transit time equation (2.12) which is given more accurately by

$$\nu = (d/v_0)(1 - \beta^2). \tag{9.3}$$

The equations for x_2 and $\dot{x}_2$ are not significantly changed.

(3a) (Continued). Equation (2.15) giving the deflection of the electron beam can be written in more useful form if the negligible term involving $(v_0/\omega L)$ is omitted and if $\cos\omega(t_1+\nu/2)$ is replaced by its approximate equal $(-1)^n\cos\omega t_1$:

$$x' = 2\beta L\left[\sin^2(\omega\nu/2) + (d/2L)^2\right]^{1/2}\sin(\omega t_1+\alpha)\ . \tag{9.4}$$

In discussing this equation it is supposed that the detection scheme involving measurement of the beam current is to be used. In this case, the condition for maximum collector current is (see Section III)

(9.5) $\sin(\omega\nu/2) = 0$ or $\omega(d/v_0)(1-\beta^2) = 2n\pi$.

This alters the equation for (e/m_0) given in Section II by placing the term $(1-\beta^2)^2$ in the numerator instead of in the denominator.

The second term in the bracket of equation (9.4) gives rise to a deflection and hence a reduction in collector current regardless of the transit time. It does not, however, affect the position of the maximum current, but obscures its precise location, thus reducing the precision by increasing the probable error of voltage adjustment. The effect is best shown graphically; Figure (12) shows this effect in terms of the constants of equation (9.4) and the width of the slit (h). The width of the collector current peak is inversely proportional to $(\beta L/h)$ as was shown in section III. The loss of a sharp maximum is of concern here and can be shown to depend on the ratio of $(d/2L)$ and the quantity $(h/2\beta L)$, that is on the magnitude of $(\beta d/h)$ (see Figure 12a).

Increase in precision requires that $(\beta L/h)$ be increased since Figure (12) shows that this decreases the peak width. However, to achieve this by increasing the field strength and hence (β) or by decreasing (h) beyond a certain limit has an undesirable effect. As shown in Figure (12b) this not only narrows the peak, but also reduces its height. The sides also depart from linearity but the peak of course still remains symmetrical. Figure (12c) shows that the increase in $(\beta L/h)$ should be achieved insofar as possible by increasing (L). However, examination of the various curves of Figure (12b) shows that if for the largest practicable value of (L), the value of $(\beta d/h)$ is less than (0.5), the precision can still be increased by increasing (β) or decreasing (h) until this factor has approximately the above value.

The values of the above constants can be most readily obtained

from the known lengths, (L) and (d), and from the observed slope of the current peak. For the apparatus described earlier these constants are given below:

$$L = 100 \text{ cm.} \qquad d = 3.0 \text{ cm.}$$

$$\beta L/h \approx 2.5 \qquad \beta d/h \approx 0.08$$

Comparison of the experimental curve shown in Figure (9) with the curves of Figure (12a) shows good agreement. Since the value of $(\beta d/h)$ is approximately (0.1) it is apparent that considerable improvement can be effected. Increase in this quantity (either by increasing (β), decreasing (h) or both) by a factor larger than five is useless, but if this factor were used, an improvement in resolution by a factor of three or four would result. To achieve the desired factor of seven, it would be necessary to further decrease the peak width by doubling the length (L). This is undesirable from the standpoint of construction and shielding, but is by no means impossible. These changes should increase the resolving power of the equipment sufficiently to permit determination of (e/m_0) with a probable error of about 1 part in 10,000.

The possibility of greater accuracy has been examined to some extent. The quantities involved in this determination have been shown to be measurable with much greater accuracy than required, except for three limitations:

(1) Correction to length (d) due to "skin effect"

(2) Correction to length (d) due to entry and exit holes

(3) Error in adjustment of voltage to proper value.

Analysis of the last effect depends of course on accurate analysis of the electron trajectories. Preliminary investigation of this has shown that the more accurate equations do not appreciably alter the condition

for a minimum deflection, but that additional disturbing terms are present. These appear to subtract from the term ($d/2L \sin \omega t_1$) thereby permitting sharper peaks and greater accuracy. However, these terms become appreciable in magnitude only if the field strength is increased to a value approximately ten times the value used. If this effect has been properly analyzed, the precision of voltage adjustment can be increased even more. Nevertheless the corrections to (d) still limit the minimum probable error due to uncertainties in these corrections. However, this minimum probable error may be substantially smaller than the value given above. The effect of these corrections can be reduced by increasing the length (d) although this will alter the voltages required for the proper transit times and will further increase the value of field strength required to minimize the effect of the term (d/2L) of equation (9.4).

The preliminary apparatus has given a value for (e/m_0) with a probable error of 4 parts in 1000. It appears that a value with probable error of about 1 part in 10,000 can be readily achieved if the field strength within the cavity is increased by a factor of about five and if the drift length (L) is doubled. It may be possible to effect a further substantial increase in accuracy by doubling the cavity length and increasing the field strength an additional amount.

APPENDIX I - SOME PROPERTIES OF A RESONANT CAVITY

The following properties of a cylindrical cavity excited in the $TM_{11}{}_0$ mode can be readily derived from Maxwell's equations. Let the radius of the cavity be (a), and its depth (d).

(1) Field configuration:

$$\bar{E} = 2\omega B_0/kc \left(J_1(k\rho) \cos(\phi+\alpha) \right) \sin(\omega t+\gamma) \quad \bar{k}_1$$

$$\bar{B} = 2B_0 \left\{ \bar{\rho}_1 \left[J_1(k\rho)/(k\rho) \right] \sin(\phi+\alpha) + \bar{\phi}_1 J_1'(k\rho) \cos(\phi+\alpha) \right\} \cos(\omega t+$$

(2) Resonant frequency:

$J_1(ka) = 0$. Hence $(ka) = 3.832$. Thus $\omega = kc = (3.832/a)c$.

(3) "Q" of cavity:

$Q = ad/(a+d)\Delta$ where Δ is the "skin depth".

(4) Power input:

$$P = \frac{\omega}{4(10)^7} \quad \frac{B_0^2 a^2 d J_0^2(ka)}{Q}$$

Here the power is in watts if the field strength is in Gauss and the dimensions are in cm.

(5) Electric field configuration near the origin:

At $\bar{\rho} = 0$ and in the direction $\phi = (\pi/2 - \alpha)$, $\bar{E} = 0$

In the direction $\phi = -\alpha$, $\bar{E} = 2\omega B_0/kc \; J_1(kx) \sin(\omega t+\gamma) \quad \bar{k}_1$

$$= \omega B_0/c \quad \sin(\omega t+\gamma) \quad (x - k^2x^3/8 + \;) \quad \bar{k}_1$$

(6) Magnetic field configuration near the origin

At $\bar{\rho} = 0$, $\bar{B} = B_0 \bar{j}_1$

In the direction $\phi = (\pi/2 - \alpha)$

$$\bar{B} = 2B_0 \; J_1(k\rho)/(k\rho) \quad \cos(\omega t+\gamma) \quad \bar{j}_1$$

$$= B_0 \cos(\omega t+\gamma) \quad (1 - k^2y^2/8 + \;) \quad \bar{j}_1$$

In the direction $\phi = -\alpha$

$$\bar{B} = 2B_0 J_1'(k\rho) \cos(\omega t+\gamma) \quad \bar{j}_1$$

$$= B_0 \cos(\omega t+\gamma) \quad (1 - 3k^2x^2/8 + \ ) \ \bar{j}_1$$

APPENDIX II - DERIVATION OF COLLECTOR CURRENT EQUATION

It is assumed that the electron beam is of uniform density, has a total intensity (I_o), a width (h), and is impinging on a slit also of width (h). The deflection of the beam from the position where it all passes through the slit is assumed to be of the form $x = x_o \sin \omega t$.

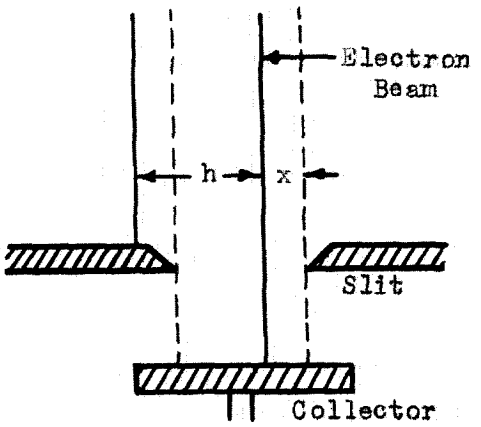

The average current through the slit can be obtained by integrating the total charge passing through the slit during a quarter period of the oscillation and dividing by the quarter period. Two cases must be considered, that where the maximum deflection (x_o) is less than (h) and that where it is greater than (h).

I. If (x_o) is less than (h).

$$I_{ave} = 2\omega/\pi \int_0^{\pi/2\omega} I \, dt = 2\omega I_o/\pi \int_0^{\pi/2\omega} (1 - x_o/h \sin \omega t) \, dt$$
$$= I_o\left(1 - \frac{2}{\pi}\frac{x_o}{h}\right).$$

II. If (x_o) is greater than (h).

$$I_{ave} = 2\omega I_o/\pi \int_0^{\sin^{-1}h/x_o} (1 - x_o/h \sin \omega t) \, dt$$
$$= I_o(2/\pi)\left[\sin^{-1}(h/x_o) + (x_o/h)\left(\sqrt{1-(h/x_o)^2} - 1\right)\right]$$

In the notation of Section III, $x_o = \beta L \sin(\omega\nu/2)$. If now we set $\gamma = x_o/h = \beta L/h \sin(\omega\nu/2)$ the equations above become:

$$I = I_o(1 - 2\gamma/\pi) \qquad \text{for } (\gamma) \text{ less than } 1$$
$$I = I_o(2/\pi)\left[\sin^{-1}(1/\gamma) - \gamma + \sqrt{\gamma^2-1}\right] \qquad \text{for } (\gamma) \text{ greater than } 1.$$

APPENDIX III - BOUNDARY EFFECT ON ELECTRON TRAJECTORIES

The problem here is to derive an expression for the difference in lateral velocity of an electron which has traversed a region of uniform field, $(\overline{B_o})$, which has perfectly sharp boundaries, and one which has traversed a region of uniform field, $(\overline{B_o})$, except near the boundaries where it falls to zero in a symmetrical manner about the value $(\overline{B_o}/2)$. That is, if the field has a value $(\overline{B_o}/2)$ at (z_o), Then the value at (z_o+z') and at (z_o-z') are $(\overline{B_o}/2+\overline{B'})$ and $(\overline{B_o}/2-\overline{B'})$ respectively. Except for the requirement that the field be symmetrical in this respect, and that the region of variation be small compared with the length of the entire region, the manner of variation is unspecified.

At a distance $d' = v_o t'$ from the boundary let the field be $(k\overline{B_o})$ "outside" of the cavity region, and $(1-k)\overline{B_o}$ "inside". Then the additional impulse imparted to an electron in the interval $\Delta t'$ by the fields not considered in the derivation of section II will be:

$$m\Delta\dot{x}_2 = I = F\,\Delta t = -\frac{ev_o}{c} B_o \left[k\cos\omega(t_1-t')\,\Delta t' - k\cos\omega(t_1+t')\,\Delta t' - k\cos\omega(t_1+\nu-t')\,\Delta t' + k\cos\omega(t_1+\nu+t')\,\Delta t'\right]$$

$$= \frac{4ev_o}{c} B_o k \sin\omega t' \sin(\omega\nu/2)\cos\omega(t_1+\nu/2)\,\Delta t'.$$

It is to be noted that this impulse varies with ν in the same manner as the expression for $\dot{x}_2$ given in section II,

$$\dot{x}_2 = 2\beta v_o \sin(\omega\nu/2)\cos\omega(t_1+\nu/2).$$

Hence the value of ν for which $\dot{x}_2$ will equal zero is no different for this case, but the coefficient which determines the rate at which $\dot{x}_2$ changes with ν is decreased by a small factor obtained by integration of the equation above.

This factor is of course 1 for a field with a sharp boundary.

Another simple case which can be readily integrated is that of a field which rises linearly from 0 to $(\overline{B_0})$ in a distance $(2v_0 \Delta\nu)$ at each boundary. In this case the factor is $\sin \omega(\Delta\nu)/ \omega(\Delta\nu)$ which is nearly 1 if $(\omega\Delta\nu)$ is a small angle. This latter requirement is equivalent to requiring that the field rise to its maximum value in a distance short compared to the length of the cavity.

APPENDIX IV - FIELD PENETRATION THROUGH A BOUNDARY

The only important cases simple enough to treat analytically are the penetration of magnetic field into a slit in an infinite plane or into a slot which is infinitely long and deep, and the penetration of magnetic field into a region below an infinitely thin sheet with a circular hole in it. Such boundaries are illustrated in Figure (10). In all cases, the magnetic field is to be uniform and parallel to the boundary at a distance from the region of disturbance, and in the first two cases is to be at right angles to the direction of the slit. The boundary condition is that $\overline{B}$ is to be parallel to the surface of the sheet or slot. The first two cases are essentially two dimensional problems and can be solved by use of conformal transformations: the last can most conveniently be treated by use of oblate spheroidal coordinates.

I. The proper transformation for the first case is

$$\frac{dz}{dz_1} = a\frac{(z_1^2 - a^2/4)}{z_1^2}$$

where the slit width is (2a).

Integration of this equation and solution for the field strength on the axis gives:

$$B = \frac{\lambda^2}{\lambda^2+1} \quad \text{where } \frac{y}{a} = \frac{\lambda}{2} - \frac{1}{2\lambda} \quad .$$

II. For the second case the transformation is

$$\frac{dz}{dz_1} = a\frac{\sqrt{1-z_1^2}}{z_1} dz_1$$

where the slit width is (2a).

The field strength on the axis can be calculated using the following equations:

$$B = \frac{\lambda}{(\lambda^2+1)} \quad \text{where} \quad \frac{V}{a} = 2/\pi \left(\sqrt{1+\lambda^2} - \operatorname{csch}^{-1} \lambda\right) .$$

III. In the three dimensional problem, the magnetostatic potential is given by the following functions of the spheroidal coordinates:

$$\Phi = B_0 P_1^1(j\zeta) P_1^1(\xi) \cos \phi + C Q_1^1(j\zeta) P_1^1(\xi) \cos \phi .$$

Evaluating the constant C by use of the boundary conditions, and substituting alternative expressions for the associated Legendre functions give:

$$\Phi = B_0 \sqrt{1+\zeta^2} \sqrt{1-\xi^2} \cos \phi \left[1 - 1/\pi(\cot^{-1}\zeta - \zeta/1+\zeta^2)\right].$$

The magnetic field can be obtained by taking derivatives of this function. Simple expressions are not obtained except on the axis, but the most important fact can be deduced from the above equation. Inserting $(-\zeta_0)$ for (ζ_0) and simplifying yield the following equations:

$$\Phi(+\zeta_0) = B_0 \sqrt{1+\zeta_0^2} \sqrt{1-\xi^2} \cos \phi \left[1 - 1/\pi(\cot^{-1}\zeta_0 - \zeta_0/1+\zeta_0^2)\right]$$

$$\Phi(-\zeta_0) = B_0 \sqrt{1+\zeta_0^2} \sqrt{1-\xi^2} \cos \phi \left[1/\pi(\cot^{-1}\zeta_0 - \zeta_0/1+\zeta_0^2)\right] .$$

The vertical component of the field is of no interest since it does not affect the motion of the electron beam. It is clear from the symmetry of the above equations that the horizontal component of the field which is perpendicular to the original field $(\overline{B_0})$ has equal but opposite values above and below the plane. This component which influences the electron motion parallel to the slits forming the beam is also of no interest. The remaining component is symmetrical about the plane of the hole where the value is $(\overline{B_0}/2)$ in the sense that the decrease of field from the value $(\overline{B_0})$ above the plane is equal to the field below the plane.

In particular, the field on the axis of symmetry has only a component parallel to $(\overline{B_0})$. This field can be readily calculated as follows:

$$B = \left.\frac{\partial \Phi}{\partial\{(1+\varsigma^2)^{1/2}(1-\varsigma^2)^{1/2}\cos\phi\}}\right|_{\varsigma=1} = B_0\left[1 - 1/\pi(\cot^{-1}\varsigma - \varsigma/1+\varsigma^2)\right] .$$

A plot of (B) on the axis for all three cases above is shown in Figure (10).

APPENDIX V - SYMBOLS AND NOTATION

a Radius of cavity ; discontinuity in boundary problem

B Magnitude of magnetic induction

c Velocity of light

d Length of cavity

e Charge of the electron

E Magnitude of electric field

f Resonant frequency of cavity

h Slit width

$\bar{I}, \bar{J}, \bar{K}$ Unit vectors along x y z axes

L Drift Length

m_0 Rest mass of the electron

n Number of cycles of cavity oscillation in electron transit time

Q Factor relating energy stored to energy loss in resonant cavity

t_1 Time at which electron enters cavity

t_2 Time at which electron leaves cavity

v_0 v_1 v_2 Electron velocities at time of entry into cavity

V Difference of potential

α Phase angle in time

β Quantity proportional to the field strength in cavity

γ Arbitrary phase angle in time

Δ Skin depth of cavity

λ Dimensionless parameter in boundary problems

ν Transit time of electron through cavity

I Potential function

ω Angular frequency of resonant cavity

REFERENCES

(1), (3) F. Kirchner: Ann d Physik: 8 (1931), Pg 975

(2) F. G. Dunnington: Phys Rev: 52 (1937), Pg 475

(4) C.T. Perry and E.L. Chaffee: Phys Rev: 36 (1930), Pg 904

(5) R. T. Birge: Rev Mod Physics: 13 (1941), Pg 233

(6) J. D. Stranathan: The Particles of Modern Physics: Pgs 101 - 146